Dissolving Microneedle Delivery of Nanoparticle Encapsulated Antigen Elicits Efficient Cross-Priming and Th1 Immune Responses by Murine Langerhans Cells

Published in:
Journal of Investigative Dermatology

Document Version:
Peer reviewed version

Queen's University Belfast - Research Portal:
Link to publication record in Queen's University Belfast Research Portal

Dissolving Microneedle Delivery of Nanoparticle Encapsulated Antigen Elicits Efficient Cross-Priming and Th1 Immune Responses by Murine Langerhans Cells

Marija Zaric, Oksana Lyubomska, Candice Poux, Mary Hanna, Maeliosa McCrudden, Bernard Malissen, Rebecca Ingram, Ultan F Power, Christopher J Scott, Ryan F Donnelly, Adrien Kissenpfennig

Dissolving Microneedle delivery of Nanoparticle encapsulated Antigen elicits efficient cross-priming and Th1 immune responses by murine Langerhans cells

*Marija Zaric[1], Oksana Lyubomska[1], Candice Poux[1], Mary Hanna[1], Maeliosa McCrudden[5], Bernard Malissen[2,3,4], Rebecca Ingram[1], Ultan F. Power[1], Christopher J. Scott[5], Ryan F. Donnelly[5], *Adrien Kissenpfennig[1]*

[1]The Centre for Infection and Immunity, School of Medicine, Dentistry and Biomedical Sciences, Queen's University Belfast, University Road, Belfast, BT9 7AE, UK.

[2]Centre d'Immunologie de Marseille-Luminy (CIML), Aix Marseille Université, UM2, Marseille, France. [3] INSERM U1104, Marseille, France. [4]CNRS UMR7280, Marseille, France

[5]School of Pharmacy, Queen's University Belfast, Lisburn Road, Belfast, BT9 7BL, UK.

Corresponding Author

*Dr Adrien Kissenpfennig

Mailing address: Centre for Infection and Immunity, School of Medicine, Dentistry and Biomedical Sciences, Queen's University Belfast, University Road, Belfast, BT9 7AE, UK

Telephone number: +44 28 90 97 2295

E-mail: a.kissenpfennig@qub.ac.uk

1

ABSTRACT

Dendritic cells (DCs) of the skin play an important role in skin-mediated immunity capable of promoting potent immune responses. We availed of polymeric dissolving microneedle (MN) arrays laden with nano-encapsulated antigen to specifically target skin DC networks. This modality of immunization represents an economic, efficient and potent means of antigen delivery directly to skin DCs, which are inefficiently targeted by more conventional immunization routes. Following MN immunization, Langerhans cells (LCs) constituted the major skin DC subset capable of cross-priming antigen-specific CD8$^+$ T cells *ex-vivo*. While all DC subsets were equally efficient in priming CD4$^+$ T cells, LCs were largely responsible for orchestrating the differentiation of CD4$^+$ IFN-γ and IL-17 producing effectors. Importantly, depletion of LCs prior to immunization had a profound effect on CD8$^+$ CTL responses *in vivo*, and vaccinated animals displayed reduced protective anti-tumour and viral immunity. Interestingly, this cross-priming bias was lost following MN immunization with soluble antigen, suggesting that processing and cross-presentation of nano-particulate antigen is favoured by LCs. Therefore, these studies highlight the importance of LCs in skin immunization strategies and that targeting of nano-particulate immunogens through dissolvable polymeric MNs potentially provides a promising technological platform for improved vaccination strategies.

2

INTRODUCTION

Elucidation of the mechanisms that underpin the functional specialization of distinct DC populations is important for the development of improved immunotherapies and the generation of DC-targeted vaccines, particularly in the skin, which represents an attractive site for vaccine delivery (Romani *et al.*, 2010). In normal epidermis, langerin (CD207)-expressing Langerhans cells (LCs) constitute the only population of professional antigen-presenting cells, while the dermis harbours three distinct CD207$^+$ DC subsets: migratory LCs, CD207$^+$CD103$^+$ and CD207$^+$CD103$^-$ dermal DCs (dDCs), in addition to two CD207$^-$ dDC subsets, characterized by differential expression of CD11b (Henri *et al.*, 2010).

Numerous studies have highlighted significant *in vivo* functional heterogeneity among skin DC populations. CD207$^+$ dDCs appear to be required for protective immunity in a number of infection and vaccination models, while the precise contribution of LCs in promoting immune responses *in vivo* remains controversial. Several studies have questioned whether LCs are required for the generation of protective antigen-specific immune responses in different mouse models (Kautz-Neu *et al.*, 2011; Ritter *at al.*, 2004; Zhao *et al.*, 2003), while studies permitting the conditional or constitutive ablation of CD207$^+$ DCs suggest that LCs instigate antigen-specific unresponsiveness or tolerance under homeostatic conditions (Schrwarz *et al.*, 2010; Henri *et al.*, 2010; Idoyaga *et al.*, 2013). Another unresolved question is whether LCs are capable of efficient cross-priming antigen *in vivo* (Romani *et al.*, 2012), with numerous models attributing this role primarily to CD207$^+$ dDCs and lymph node (LN) resident CD8$^+$ DCs (Igyarto and Kaplan, 2013). LCs have been shown to stimulate type 2 T-helper (Th) cell responses (Nagao *et al.*,

3

2009; Stoecklinger *et al.*, 2011; Hauser *et al.*, 1989), however, LCs have been shown to also evoke Th1 cell responses or activate Th17 cells (Duraisingham *et al.*, 2009; Mathers *et al.*, 2009; Igyarto *et al.*, 2011).

In this study, we entrapped the model antigen, ovalbumin (OVA), into Poly-D-L-lactide-co-glycolide (PLGA) nanoparticles (NPs), as these particles were previously shown to have strong immune-modulatory properties and activate DCs to induce efficient T-cell immune responses (Gutierro *et al.*, 2002; Jaganathan *et al.*, 2006). Previous studies have demonstrated the capacity of model protein antigens, inactivated or subunit vaccines to prime adaptive immunity when delivered *via* MN arrays (Sullivan *et al.*, 2010; Kim *et al.*, 2012). To this end, we employed biodegradable polymeric dissolvable MNs to specifically target NP-encapsulated antigen to DCs within the different skin compartments to enhance their activation and promote adaptive immunity. Recently, we demonstrated that MN-mediated delivery of nano-encapsulated antigen efficiently targeted skin DCs, which in turn induced efficient T cell responses (Zaric *et al.*, 2013). However, the contribution of individual skin DC subsets in the induction of immune responses using our vaccination strategy was not examined in detail. Utilising skin DC ablation models, we demonstrate that following MN-mediated NP-immunization, LCs are central in cross-priming antigen *in vivo* and inducing Th1 and Th17 immune responses by antigen-specific CD4^{+} T cells. Importantly, we highlight the prerequisite for LCs to generate both antigen-specific anti-tumour and anti-viral immune responses following antigen-NPs MN immunization.

RESULTS

LCs are the major population capable of cross-priming CD8^{+} T cells

4

To determine the contribution of specific DC subsets following intradermal immunization, dissolvable MNs containing OVA encapsulated nanoparticles (OVA-NPs) were applied to Lang^{eGFP} mouse ears, and DC subsets from pooled auricular LNs were purified by FACS 24h and 72h post-immunization. Skin-derived DCs (CD11c$^+$MHCII^{high}CD8$^-$) were sorted into distinct DC subsets on the basis of eGFP, CD103 and Ep-CAM expression (**Fig. S1**). Following co-culture of purified skin DCs with CFSE-labelled OVA-specific OT-I CD8$^+$ or OT-II CD4$^+$ T cells, we found that LCs constituted the major subset able to cross-present OVA-NPs, although a low degree of antigen presentation to CD8$^+$ OT-I T cells was mediated by other dDC subsets (**Fig. 1a-b**). In contrast, all skin DC subsets were equally able to efficiently activate and induce CD4$^+$ OT-II cell proliferation *in vitro* (**Fig. 1c-d**). Due to their observed slower migration to the draining LNs (Kissenpfennig *et al.*, 2005), LCs-induced OT-I and OT-II T cell proliferation peaked at 72h post MN vaccination. Importantly, delivery of TRITC NPs *via* MN application demonstrated that NPs were equally taken up by all skin DC subsets *in vivo* (**Fig. S2**). Therefore, LCs are the predominant skin DC subset that contribute to cross-priming of naïve antigen-specific CD8$^+$T cells following immunization with dissolvable MNs laden with antigen-encapsulated NPs. However, no observed bias by the specific skin DC subsets could be discerned for antigen presentation and/or activation of CD4$^+$ T-cells.

LCs are necessary for optimal cross-presentation *in vivo*

To substantiate our findings with *ex-vivo* skin DCs in an *in vivo* system, we employed our Lang^{hDTR} model and depleted CD207$^+$ DCs prior to immunization (Kissenpfennig *et al.*, 2005). To deplete LCs only, Lang^{hDTR} mice were treated *i.p.* with a single dose

5

of diphtheria toxin (DT) 7 days prior to MN immunization, or a supplementary DT dose was given one day prior to immunization to deplete both LCs and CD207^{+} dDC, consistent with previously published studies (**Fig. S3**) (Poulin *et al.*, 2007; Bursch *et al.*, 2007; Ginhoux *et al.*, 2007). One day prior to blank NP (b-NP) or OVA-NP immunization, DT untreated or treated Lang[hDTR] mice were adoptively transferred with CFSE-labelled CD8^{+} T cells purified from CD45.1 congenic OT-I mice. Expansion of donor CD8^{+} cells in auricular LNs was analysed 7 days post MN immunization. As expected, efficient expansion of antigen-specific CD45.1^{+}CD8^{+} T cells was detected following immunization with OVA-NPs compared to mice immunized with b-NPs. In contrast, expansion of OVA-specific CD8^{+} T cells was significantly reduced in Lang[hDTR] mice receiving either DT dosing regimes (**Fig. 2a**). Interestingly, all skin DC subsets had the capacity to induce efficient IFN-γ production among proliferating OT-I cells, notwithstanding that absolute numbers of IFN-γ[+]OT-I T cells were significantly reduced in the absence of LCs (**Fig. 2b**).

These observations were substantiated in a genuine *in vivo* model by examining the expansion of endogenous OVA-specific CD8^{+} T cells following MN immunization with b-NPs or OVA-NPs. Utilising the same immunization and depletion protocol described above, isolated auricular LN cells were stained with OVA$_{257-264}$/H-2K[b] pentamers specific for the SIINFEKL epitope of OVA protein two weeks post-immunization. MN immunization with OVA-NPs resulted in increased percentages and total numbers of OVA-specific CD8^{+} T cells in DT-untreated mice compared to mice that had received one or two doses of DT prior to immunization (**Fig. 2c**), reaffirming the requirement for LCs for optimal cross-presentation of nano-encapsulated antigen following MN intradermal immunization.

6

LCs promote Th1 and Th17 CD4$^+$ T cell differentiation

To examine T helper immune responses by different skin-derived DC subsets, we adoptively transferred CD45.1$^+$CD4$^+$ OT-II T cells into Lang^{hDTR} mice prior to DT treatment and MN immunization. No difference in total numbers of donor OT-II cells was observed between mice with LCs, and mice lacking LCs only, or both LCs and CD207$^+$ dDCs (**Fig. 3a-b**), confirming that both CD207$^+$ and CD207$^-$ dDCs were equally capable of presenting OVA-NPs and activating CD4$^+$ T helper cells. The cytokine profile of expanded CD45.1$^+$OT-II T cells revealed that the polarisation of IFN-γ and IL-17A-producing cells necessitated the presence of LCs (**Fig. 3c-d**), while only a few OT-II cells polarized towards IL-4-producing Th2 cells. Interestingly, in the absence of LCs, the number of donor OT-II cells producing IL-4 was significantly elevated. Of note, we did not observe any notable difference in the induction of Foxp3-producing OT-II T cells in our model. Therefore, the absence of LCs has a profound effect on the development of Th1 and Th17 cells following MN-mediated delivery of nano-particulate antigen.

LCs are necessary for efficient anti-tumour responses following microneedle immunization

We further examined the contribution of LCs in antigen-specific anti-tumour immune responses. Utilising the same depletion and immunization strategy as in previous experiments, Lang^{hDTR} mice were challenged 3 weeks post MN-vaccination with B16.OVA tumour cells, and tumour growth was monitored thereafter. As expected,

DT-untreated Lang^{hDTR} mice immunized with OVA-NPs were protected against tumour challenge, while all mice immunized with b-NPs exhibited expected tumour growth. In OVA-NPs immunized mice depleted of LCs only, or both LCs and CD207$^+$ dDCs, tumours grew at a reduced rate and mice survived longer compared to b-NPs immunized mice (**Fig. 4a-b**), suggesting that all skin DCs contribute to anti-tumour immunity following MN-mediated intradermal immunization. However, mice with LCs present developed smaller tumours and survived significantly longer than DT-treated animals (**Fig. 4a-b**), highlighting the importance of LCs for optimal anti-tumour immunity in this model. Furthermore, staining of tumour cell suspensions with OVA$_{257-264}$/H-2K^b pentamers identified a clear population of OVA-specific tumour-infiltrating CD8$^+$ T cells in DT-untreated mice, which was found to be 3-5 fold reduced in mice lacking LCs or all CD207$^+$ skin DCs at the time of OVA-NPs immunization (**Fig. 4c**). Similarly, the percentages of tumour-infiltrating total CD8$^+$ T cells were increased in DT-untreated mice compared to mice that had received one or two doses of DT prior to immunization (**Fig. S4**).

To determine the contribution of skin DC subsets in evoking therapeutic anti-tumour immunity, DT treated and untreated Lang^{hDTR} mice were first injected into the flank with B16.OVA tumour cells, and on days 4 and 9 following tumour inoculation they were immunized with MNs (**Fig. S5**). Only tumours from OVA-NPs immunized DT-untreated animals were significantly affected. These tumours were notably smaller compared to tumours from b-NPs immunized mice 15 days post-tumour inoculation, suggesting that the presence of all skin DC subsets in the skin at the time of immunization is necessary for robust anti-tumour activity in a therapeutic setting (**Fig. 4d**). Mice survival determined by tumour volume end-point between different experimental groups found that irrespective of the presence of LCs, treatments with

8

OVA-NPs MNs prolonged overall survival of mice compared to mice treated with b-NPs MNs. However, survival was further improved if LCs were present in the skin at the time of OVA-NPs MN immunization (**Fig. 4e**).

LCs are required for effective anti-viral responses following microneedle immunization

To test the capacity of different skin-derived DC subsets to promote protective viral immunity following MN-mediated vaccination in a murine para-influenza virus model, we utilized a recombinant Sendai virus expressing an ovalbumin/red fluorescent fusion protein (SeV^{OVATdT}) (Zaric *et al.*, 2013). Lang^{hDTR} mice were either untreated or treated with DT, immunized with b-NPs or OVA-NPs, and three weeks later intranasally challenged with SeV^{OVATdT}. All b-NPs immunized animals did not survive beyond 6 days post-challenge (**Fig. 5a**). When depleted of LCs, OVA-NPs immunized mice presented with significantly reduced survival compared to DT-untreated controls that all survived the challenge. Analysis of whole lung cell suspensions revealed significantly increased percentages of SeV^{OVATdT} positive cells in b-NPs immunized mice compared to untreated OVA-NPs immunized animals. Furthermore, there was a 3-5 fold increase in percentages of SeV^{OVATdT} positive cells in mice lacking LCs, or both LCs and CD207$^+$ dDCs compared to mice with their full complement of skin DCs (**Fig. 5b-c**). Lung viral titre measurements confirmed significantly higher viral titres in DT-treated OVA-NPs immunized mice compared to DT-untreated mice, where viral titres were below detection levels (**Fig. 5d**).

Analysis of lung cell suspensions 6 days post-challenge revealed that OVA-specific CD8$^+$ T cells could consistently be detected in the lungs of OVA-NPs immunized

9

mice (**Fig. 5e**), while this population was 2-3 fold reduced when LCs or all CD207$^+$-expressing skin DCs were depleted at the time of MN immunization. We did not observe any significant differences in the ability of LCs, or CD207$^+$ and CD207$^-$ dDC subsets to activate IFN-γ and/or Granzyme B expressing CD8$^+$ T cells, as the proportion of IFN-γ^+ and Granzyme B$^+$ OVA-specific T cells remained similar between the different DT treatment groups (**Fig. 5f**). Collectively, these results demonstrate that the presence of LCs in the skin at the time of immunization with MNs laden with antigen- NPs is essential for promoting the activation and expansion of antigen-specific CD8$^+$ T cells contributing to the complete protection against pulmonary viral challenge.

Effective LCs cross-presentation is dependent on nano-encapsulation of antigen

Although our results suggest that LCs represented the predominant DC subset capable of cross-priming nano-encapsulated antigen following MN delivery, it was unclear whether preferential activation of antigen-specific CD8$^+$ T cells by LCs occurred as a consequence of antigen nano-encapsulation or MN-mediated antigen delivery. Therefore, we directly compared the ability of different skin-derived DC subsets to cross-present antigen delivered by MNs, as either a nano-particulate or a non-nano-particulate formulation. MNs containing either OVA-NPs or the comparable amount of OVA were applied to mouse ears, and DC subsets from auricular LNs were purified by FACS 72h post-immunization as previously described. Following co-culture of DC subsets with CFSE-labelled OT-I cells, we confirmed that nano-particulate antigen was again predominantly cross-presented by LCs. In contrast,

10

MN delivery of soluble OVA demonstrated that CD207+CD103+ dDCs were the major population responsible for antigen cross-presentation (**Fig. 6a**). All other skin-derived DC subsets, including LCs, can to some extent, cross-present soluble antigen, however, the degree of T cell activation by these subsets was significantly reduced in comparison to CD207+CD103+ dDCs (**Fig. 6b**). Importantly, these experiments suggest that the physical nature of the immunogen could impact the functional specialisation of skin DCs following intradermal immunization. CD207+CD103+ dDCs were found to have a superior ability to cross-prime soluble antigen, while cross-presentation of nano-encapsulated antigen was strongly favoured by LCs.

DISCUSSION

On-going research in skin DC immunobiology, together with development of new technologies for manipulating DCs, highlight their promising potential in the prevention and treatment of various infectious diseases and cancer (Romani *et al.*, 2010). However, skin DCs populations are heterogeneous, composed of phenotypically and functionally diverse subsets and ensuing immune responses may be influenced by the subset of DC involved. Several studies designed to test LC-mediated cross-presentation *in vitro* or *ex vivo* have confirmed their ability to efficiently present exogenously acquired antigen to antigen-specific CD8+ T cells (Klechevsky *et al.*, 2010, Stoitzner *et al.*, 2006). In line with Stoitzner *et al.*, we show here that LCs are also able to efficiently cross present nano-encapsulated antigen to OT-I T cells *ex vivo* following MN-mediated OVA-NPs immunization.

Extensive data to demonstrate LC cross-presentation *in vivo* has been limited (Igyarto and Kaplan, 2013). To date, cross-presentation of cutaneous antigen has

11

been shown to be dependent on CD207^{+} CD103^{+} dDCs (Stoecklinger *et al.*, 2011, Bobr *et al.*, 2010), whilst we observed only modest antigen cross-priming by dDCs following NPs-MN immunization. In addition, we cannot completely exclude that monocyte-derived infiltrating inflammatory DCs (Cheong *et al.*, 2010) played an additional role in cross-priming. However, they have been shown to be poorly represented in the skin DC migratory fraction of lymph nodes, and had reduced capacity for naïve T cell activation *in vivo* (Tamoutounour *et al.*, 2013). In contrast to nano-encapsulated antigen, our data suggests that delivery of soluble antigen was most efficiently presented by CD207^{+} CD103^{+} dDCs rather than LCs. Indeed, the ability of CD207^{+}CD103^{+} dDCs to cross present skin-borne antigens to CD8^{+} T cells have been confirmed in several models, such as keratinocyte-restricted expression of OVA and infection models of Leishmaniasis, *Candida albicans,* HSV *and* Vaccinia virus (Henri *et al.*, 2010, Brewig *et al.*, 2009, Igyarto *et al.*, 2011, Bedoui *et al.*, 2009, Seneschal *et al.*, 2014).

The specific downstream intracellular mechanisms following PGLA-NP uptake, antigen processing and presentation by DCs and their activation in our vaccination model remains poorly understood. PLGA NPs have been shown to specifically activate the NLRP3 inflammasome (Yang *et al.*, 2013, Sharp *et al.*, 2009). Microneedle-mediated PLGA-NPs vaccination likely activates DC inflammasome signaling pathways and this could bias the cross-priming capability of LCs. Furthermore, a possible role of Birbeck's granules, a unique organelle of LCs, in controlling intracellular fate of particulate antigens cannot be dismissed and further investigation into PLGA-NP LC compartmentalization following uptake and induced activation of LCs is warranted.

A recent study, utilising Na-CMC/sucrose dissolvable MN arrays loaded with live recombinant adenovirus vector or Texas Red-Dextran demonstrated that CD8^{+} T cell immune responses to adeno-viral vectors or uptake of Texas Red-Dextran was largely attributed to the CD11b^{+}CD207^{-} dDC subset (Bachy *et al.*, 2013). Uptake of particulate antigens by DCs is dependent on several antigen-associated properties, such as size, shape, surface charge, hydrophobicity/hydrophilicity, as well as receptor interactions. Indeed, without specific recognition, PLGA-NPs are naturally targeted to DCs through phagocytosis, while adenovirus viral uptake has been shown to be receptor mediated through clathrin-mediated endocytosis and protein kinase C dependent macro-pinocytosis (Hamdy *et al.*, 2011; Meier and Greber, 2003). Likewise, subsequent activation of innate signalling pathways following viral or PLGA NPs internalisation may differ. Interestingly, a recent study demonstrated that following plasmid DNA intradermal vaccination, CD8^{+} T cell cross-priming was largely instigated by infiltrating, second generation antigen-expressing LCs (Elnekave *et al.*, 2014). Therefore, the perceived defined functional allocations among distinct skin DC subsets may not necessarily exist, but rather the underlying mechanisms that govern antigen processing, presentation and activation of DCs may influence their subsequent functional properties and the net immune response.

MN delivery of antigen-NPs to skin DCs led to efficient priming of antigen-specific CD4^{+} T cells, irrespective of the presence of LCs. However, LCs were primarily required for Th1 and Th17 development. Similarly, it has been shown that direct presentation of *C. albicans*-derived antigen by LCs was necessary for the generation of antigen-specific Th17 effectors (Igyarto *et al.*, 2011). Contrary, Fujita and co-workers showed that LCs induced IL-22 producing CD4^{+} T cells, that at the same time, lacked the expression of IL-17 and IFN-γ (Fujita *et al.*, 2009). Therefore, the

13

importance of LCs in maintaining mucosal homeostasis, and for Th17 effector responses in our immunization modality would require further confirmation in an appropriate pathogenic model.

Finally, we demonstrate that LCs are necessary for the induction of protective antigen-specific anti-viral and anti-tumour immunity. The absence of LCs had a dramatic effect on the ability of Sendai infected animals to efficiently clear pulmonary viral infection. This is supported by the observation that selective depletion of LCs *in vivo* at the time of MN vaccination was sufficient to significantly diminish the expansion of antigen-specific infiltrating CD8$^+$ T cells, confirming that dDCs had a secondary contributory role in cross-priming nano-encapsulated antigen. However, dDCs subsets still mediated some delay in tumour growth and prolonged mice survival. In mice immunised with OVA-NPs and depleted of LCs, or both LCs and CD207+ dDCs, tumours grew at a significantly decreased rate and mice survived longer compared to b-NPs immunised mice suggesting that dDCs were in part necessary for effective anti-tumour immunity. Indeed, it has recently been shown that CD207$^-$CD11b$^-$ dDCs may be an important contributor to the cutaneous immune environment (Mollah *et al.*, 2014). Moreover, depletion of both LCs and CD207$^+$dDCs showed an appreciable trend in increased tumour volumes and inferior survival in comparison to mice lacking only LCs, indicating that CD207$^+$ dDCs may beneficially contribute to anti-tumour immunity. Therefore, whether LCs alone are sufficient to induce this anti-tumour and anti-viral response or synergy with other DC subsets is required remains to be determined.

Importantly, the fact that tumour and viral challenges were performed 3 weeks post-immunization indicates that LCs were also involved in the induction of memory response. Indeed, we have previously confirmed that OVA-NPs MN immunization

14

induced antigen specific memory response in mice challenged with tumour cells 3 weeks post vaccination (Zaric *et al.*, 2013). However, more long-term challenge studies are required to confirm this observation.

Despite changing paradigms, LCs remain an essential cell in the immune system of the skin, at least in the context of antigen-NPs delivery through MNs. Emerging nano-technological advances in drug delivery coupled with self-disabling, biodegradable, dissolving MN arrays offers an exciting prospect for delivery of antigens to easily accessible skin DC populations to improve vaccine efficacy. Therefore, these results provide a strong rationale for more in-depth exploration of therapies based on MN-mediated antigen-NP targeting of LCs for the treatment of infectious diseases and tumours.

MATERIALS AND METHODS

Full details of methods are described in SI Materials and Methods.

Fabrication of NPs-Loaded MNs

MNs prepared from aqueous blends of 20% w/w PMVE/MA were fabricated using laser-engineered silicone micro-mould templates (Donnelly *et al.*, 2011). MN arrays (19×19 array, 600 µm height) containing PLGA NPs were prepared as previously described (Zaric *et al.*, 2013).

Mice

Transgenic mice, including Lang^{eGFP} reporter mice, Lang^{hDTR} mice (Kissenpfennig *et al.*, 2005), OT-I and OT-II mice (The Jackson Lab, USA) (Hogquist *et al.*, 1994; Barnden *et al.*, 1998) on a congenic CD45.1 C57BL/6 background were housed under specific pathogen-free conditions. All mice employed for experiments were between 6 to 10 weeks old, age and sex matched and were sanctioned in accordance with the UK Home Office and approved by Queen's University Belfast Animal Welfare and Ethical Review Board.

MN immunization

MNs containing 10 µg OVA encapsulated NPs or b-NPs, or soluble OVA were applied to the dorsal side of both ears. The MNs were held in place for at least 5 min and then removed.

Depletion of LCs or CD207$^+$ dDCs

For systemic *in vivo* depletion of CD207$^+$ DCs, Lang^{hDTR} mice were injected *i.p.* with 1µg Diphtheria Toxin (DT) (Quadratec Diagnostics Ltd, UK) using the specified timing of application.

Reagents for Flow Cytometry

Surface marker expression was assessed by flow cytometry using fluorochrome-conjugated antibodies (BD Biosciences and eBioscience, UK) and PE-labelled K^b/SIINFEKL pentamers were purchased from ProImmune, UK.

***In vivo* proliferation assays**

16

Mice were injected *i.v.* with 10^6 CFSE-labelled OT-I or OT-II T cells, 24 hours prior to MN immunization. Mice were sacrificed 7 days following MN application, and auricular lymph nodes were harvested for FACS analysis.

Ex-vivo proliferation assay

DCs sorted from the auricular LNs 24h or 72h post-MN immunization were co-cultured in triplicates with CFSE-labelled OVA-specific OT-I or OT-II T cells for 60h in a 1:10 ratio, and proliferation of T cells was measured by the decrease of CFSE fluorescence intensity.

Tumour challenge

Three weeks following MN immunization, mice were injected s.c. into the flank with 10^5 B16.OVA tumour cells (Brown *et al.*, 2001; kindly provided by P Stoitzner, Innsbruck). Tumour size was assessed by measuring the short and long tumour diameters using digital callipers. Measurements were stopped when tumour diameter reached maximum allowed dimension of 20 mm and mice had to be euthanized, according to UK Home Office guidelines and Queens University Belfast ethical review committee guidelines.

Challenge of mice with recombinant Sendai virus-OVA-TdT (SeV^OVA-TdT)

Experimental groups of mice were challenged 3 weeks after MN immunization by intranasal instillation of 2×10^6 pfu SeV^OVA-TdT (Zaric *et al.*, 2013) in 30 µl of PBS and monitored for up to 7 days.

Statistical analysis

17

Bars in figures show the mean ± SEM. All numerical data were analyzed for significal differences between groups by analyses of variance (ANOVA) with Prism software 5.0 (GraphPad Software, Inc.) Probability values are expressed as the following: ∗∗∗, $p < 0.001$; ∗∗, $p < 0.01$; and ∗, $p < 0.05$.

Conflict of interest

The authors state no conflict of interest.

Acknowledgements

References:

Bachy V, Hervouet C, Becker PD, *et al* (2013). Langerin negative dendritic cells promote potent CD8+ T-cell priming by skin delivery of live adenovirus vaccine microneedle arrays. *Proc Natl Acad Sci U S A* 110: 3041-6.

Barnden MJ, Allison J, Heath WR, *et al* (1998). Defective TCR expression in transgenic mice constructed using cDNA-based alpha- and beta-chain genes under the control of heterologous regulatory elements. *Immunol Cell Biol* 76: 34-40.

Bedoui S, Whitney PG, Waithman J, *et al* (2009). Cross-presentation of viral and self antigens by skin-derived CD103+ dendritic cells. *Nat Immunol* 10: 488-95.

Bobr A, Olvera-Gomez I, Igyarto BZ, *et al* (2010). Acute ablation of langerhans cells enhances skin immune responses. *J Immunol* 185: 4724-8.

Brewig N, Kissenpfennig A, Malissen B, *et al* (2009). Priming of CD8+ and CD4+ T cells in experimental leishmaniasis is initiated by different dendritic cell subtypes. *J Immunol* 182: 774-83.

Brown DM, Fisher TL, Wei C, *et al* (2001). Tumours can act as adjuvants for humoral immunity. *Immunology* 102: 486-97.

Bursch LS, Wang L, Igyarto B, *et al* (2007). Identification of a novel population of langerin+ dendritic cells. *J Exp Med* 204: 3147-56.

Cheong C, Matos I, Choi JH, *et al* (2010). Microbial stimulation fully differentiates monocytes to DC-SIGN/CD209(+) dendritic cells for immune T cell areas. *Cell* 143: 416-29.

Donnelly RF, Majithiya R, Singh TR*, et al* (2011). Design, optimization and characterisation of polymeric microneedle arrays prepared by a novel laser-based micromoulding technique. *Pharm Res* 28: 41-57.

Duraisingham SS, Hornig J, Gotch F*, et al* (2009). TLR-stimulated CD34 stem cell-derived human skin-like and monocyte-derived dendritic cells fail to induce Th17 polarization of naive T cells but do stimulate Th1 and Th17 memory responses. *J Immunol* 183: 2242-51.

Elnekave M, Furmanov K, Shaul Y*, et al* (2014). Second-generation langerhans cells originating from epidermal precursors are essential for CD8+ T cell priming. *J Immunol* 192: 1395-403.

Fujita H, Nograles KE, Kikuchi T*, et al* (2009). Human langerhans cells induce distinct IL-22-producing CD4+ T cells lacking IL-17 production. *Proc Natl Acad Sci U S A* 106: 21795-800.

Ginhoux F, Collin MP, Bogunovic M*, et al* (2007). Blood-derived dermal langerin+ dendritic cells survey the skin in the steady state. *J Exp Med* 204: 3133-46.

Gutierro I, Hernandez RM, Igartua M*, et al* (2002). Size dependent immune response after subcutaneous, oral and intranasal administration of BSA loaded nanospheres. *Vaccine* 21: 67-77.

Hamdy S, Haddadi A, Hung RW*, et al* (2011). Targeting dendritic cells with nano-particulate PLGA cancer vaccine formulations. *Adv Drug Deliv Rev* 63: 943-55.

Hauser C, Snapper CM, Ohara J*, et al* (1989). T helper cells grown with hapten-modified cultured langerhans' cells produce interleukin 4 and stimulate IgE production by B cells. *Eur J Immunol* 19: 245-51.

Henri S, Guilliams M, Poulin LF*, et al* (2010). Disentangling the complexity of the skin dendritic cell network. *Immunol Cell Biol* 88: 366-75.

Henri S, Poulin LF, Tamoutounour S*, et al* (2010). CD207+ CD103+ dermal dendritic cells cross-present keratinocyte-derived antigens irrespective of the presence of langerhans cells. *J Exp Med* 207: 189-206.

Hogquist KA, Jameson SC, Heath WR*, et al* (1994). T cell receptor antagonist peptides induce positive selection. *Cell* 76: 17-27.

Idoyaga J, Fiorese C, Zbytnuik L*, et al* (2013). Specialized role of migratory dendritic cells in peripheral tolerance induction. *J Clin Invest*.

Igyarto BZ, Haley K, Ortner D*, et al* (2011). Skin-resident murine dendritic cell subsets promote distinct and opposing antigen-specific T helper cell responses. *Immunity* 35: 260-72.

Igyarto BZ, Kaplan DH (2013). Antigen presentation by langerhans cells. *Curr Opin Immunol* 25: 115-9.

Jaganathan KS, Vyas SP (2006). Strong systemic and mucosal immune responses to surface-modified PLGA microspheres containing recombinant hepatitis B antigen administered intranasally. *Vaccine* 24: 4201-11.

Kautz-Neu K, Noordegraaf M, Dinges S*, et al* (2011). Langerhans cells are negative regulators of the anti-leishmania response. *J Exp Med* 208: 885-91.

Kim YC, Park JH, Prausnitz MR (2012). Microneedles for drug and vaccine delivery. *Adv Drug Deliv Rev* 64: 1547-68.

Kissenpfennig A, Henri S, Dubois B*, et al* (2005). Dynamics and function of langerhans cells in vivo: Dermal dendritic cells colonize lymph node areas distinct from slower migrating langerhans cells. *Immunity* 22: 643-54.

Klechevsky E, Morita R, Liu M*, et al* (2008). Functional specializations of human epidermal langerhans cells and CD14+ dermal dendritic cells. *Immunity* 29: 497-510.

Mathers AR, Janelsins BM, Rubin JP*, et al* (2009). Differential capability of human cutaneous dendritic cell subsets to initiate Th17 responses. *J Immunol* 182: 921-33.

Meier O, Greber UF (2003). Adenovirus endocytosis. *J Gene Med* 5: 451-62.

Mollah SA, Dobrin JS, Feder RE*, et al* (2014). Flt3L dependence helps define an uncharacterized subset of murine cutaneous dendritic cells. *J Invest Dermatol* 134: 1265-75.

Poulin LF, Henri S, de Bovis B*, et al* (2007). The dermis contains langerin+ dendritic cells that develop and function independently of epidermal langerhans cells. *J Exp Med* 204: 3119-31.

Ritter U, Meissner A, Scheidig C*, et al* (2004). CD8 alpha- and langerin-negative dendritic cells, but not langerhans cells, act as principal antigen-presenting cells in leishmaniasis. *Eur J Immunol* 34: 1542-50.

Romani N, Brunner PM, Stingl G (2012). Changing views of the role of langerhans cells. *J Invest Dermatol* 132: 872-81.

Romani N, Thurnher M, Idoyaga J*, et al* (2010). Targeting of antigens to skin dendritic cells: Possibilities to enhance vaccine efficacy. *Immunol Cell Biol* 88: 424-30.

Schwarz A, Noordegraaf M, Maeda A*, et al* (2010). Langerhans cells are required for UVR-induced immunosuppression. *J Invest Dermatol* 130: 1419-27.

Seneschal J, Jiang X, Kupper TS (2014). Langerin+ dermal DC, but not langerhans cells, are required for effective CD8-mediated immune responses after skin scarification with vaccinia virus. *J Invest Dermatol* 134: 686-94.

Sharp FA, Ruane D, Claass B*, et al* (2009). Uptake of particulate vaccine adjuvants by dendritic cells activates the NALP3 inflammasome. *Proc Natl Acad Sci U S A* 106: 870-5.

Stoecklinger A, Eticha TD, Mesdaghi M*, et al* (2011). Langerin+ dermal dendritic cells are critical for CD8+ T cell activation and IgH gamma-1 class switching in response to gene gun vaccines. *J Immunol* 186: 1377-83.

Stoitzner P, Tripp CH, Eberhart A*, et al* (2006). Langerhans cells cross-present antigen derived from skin. *Proc Natl Acad Sci U S A* 103: 7783-8.

Sullivan SP, Koutsonanos DG, Del Pilar Martin M*, et al* (2010). Dissolving polymer microneedle patches for influenza vaccination. *Nat Med* 16: 915-20.

Tamoutounour S, Guilliams M, Montanana Sanchis F*, et al* (2013). Origins and functional specialization of macrophages and of conventional and monocyte-derived dendritic cells in mouse skin. *Immunity* 39: 925-38.

Touzelet O, Loukili N, Pelet T, *et al* (2009). De novo generation of a non-segmented negative strand RNA virus with a bicistronic gene. *Virus Res* 140: 40-8.

Yang M, Hearnden CH, Oleszycka E, *et al* (2013). NLRP3 inflammasome activation and cytotoxicity induced by particulate adjuvants. *Methods Mol Biol* 1040: 41-63.

Zaric M, Lyubomska O, Touzelet O, *et al* (2013). Skin dendritic cell targeting via microneedle arrays laden with antigen-encapsulated poly-d,l-lactide-co-glycolide nanoparticles induces efficient antitumour and antiviral immune responses. *ACS Nano* 7: 2042-55.

Zhao X, Deak E, Soderberg K, *et al* (2003). Vaginal submucosal dendritic cells, but not langerhans cells, induce protective Th1 responses to herpes simplex virus-2. *J Exp Med* 197: 153-62.

Figure Legends

Figure 1: All skin-derived DC subsets present antigen to CD4$^+$ T cells, but LCs are the major population capable of cross-priming CD8$^+$ T cells *ex-vivo*. Mice (n=20) were immunized through MNs with OVA-NPs, and following 24h or 72h defined subsets of DCs from auricular LNs were purified by FACS. 5x10^4 OVA-specific CD8$^+$ or CD4$^+$ T cells were co-cultured in triplicates with 5x10^3 DCs of each subset for 60h. **a**) Representative histograms of CFSE dilutions of OT-I cell proliferation. **b**) Bars graphs representing the percentage of proliferating OT-I T cells. **c**) Representative histograms of CFSE dilutions of OT-II cell proliferation. **d**) Bars graphs representing the percentage of proliferating OT-II T cells. Data have been pooled from two separate experiments.

Figure 2: LCs are the major skin DC subset capable of antigen cross-presentation *in vivo* Lang^{hDTR} mice that were either untreated (DT-) or treated with DT once (DT+) or twice (DT++), received *i.v.* 10^6 CFSE-labelled, CD45.1 OT-I cells. Mice were immunized with b-NPs or OVA-NPs the following day and skin-draining LNs were harvested 7 days later. **a**) Percentages and total numbers of CD45.1$^+$OT-I cells recovered within each experimental group are shown. **b**) CFSE and expression of IFN-γ among CD8$^+$CD45.1$^+$ cells (*left panel*) and total numbers of IFN-γ producing OT-I cells within each group are shown (*right panel*). **c**) Percentages and total numbers of endogenous OVA$_{257-264}$/H2K^{b+}CD8$^+$ T cells detected in the auricular LNs among different experimental groups are shown. All flow cytometry dot plots represent an individual mouse from each experimental group obtained in one out of three separate experiments.
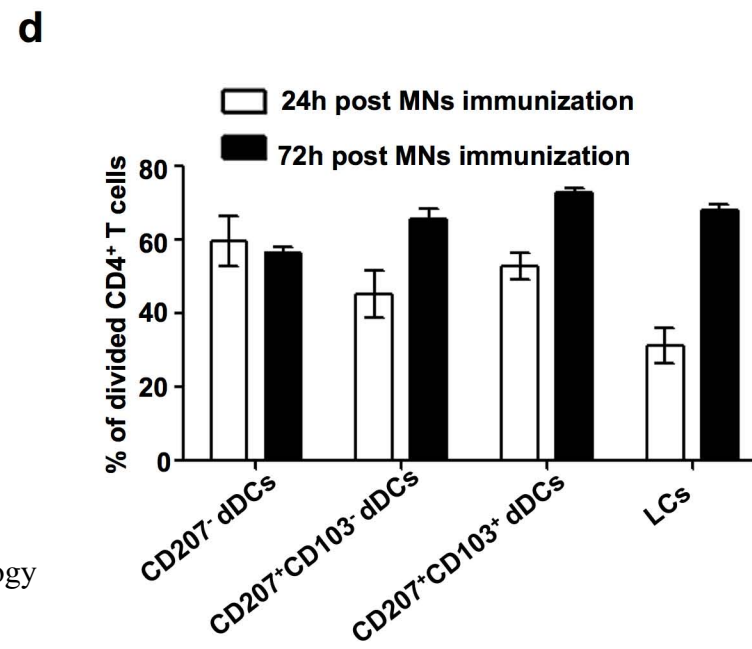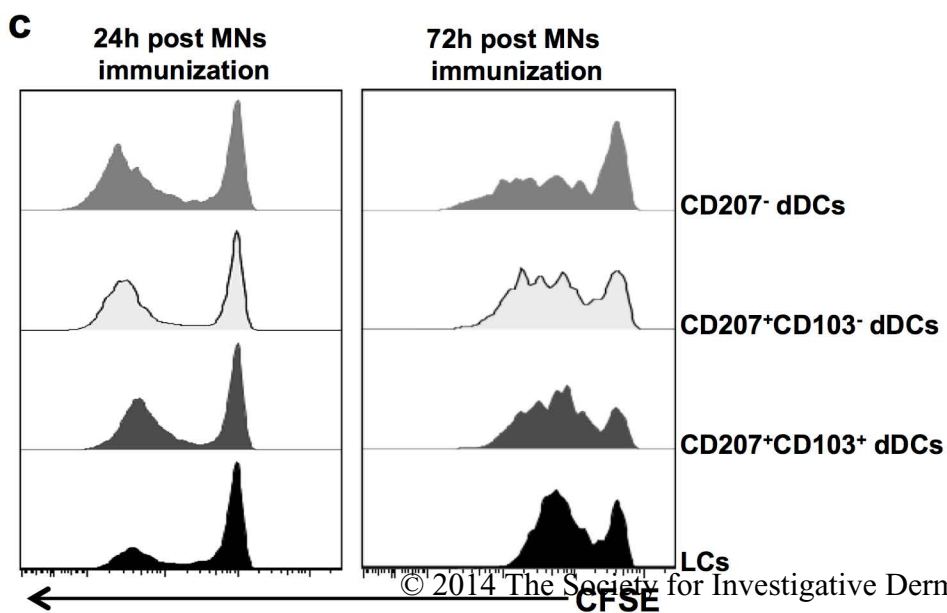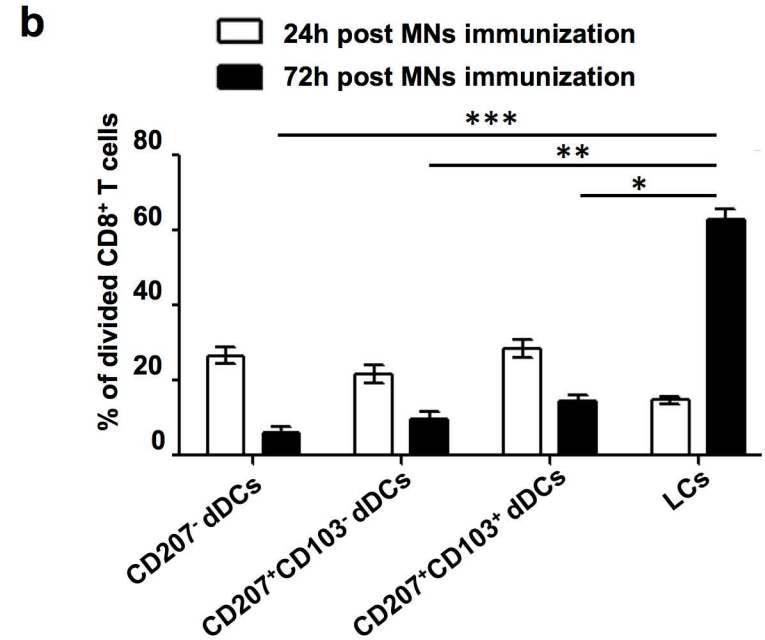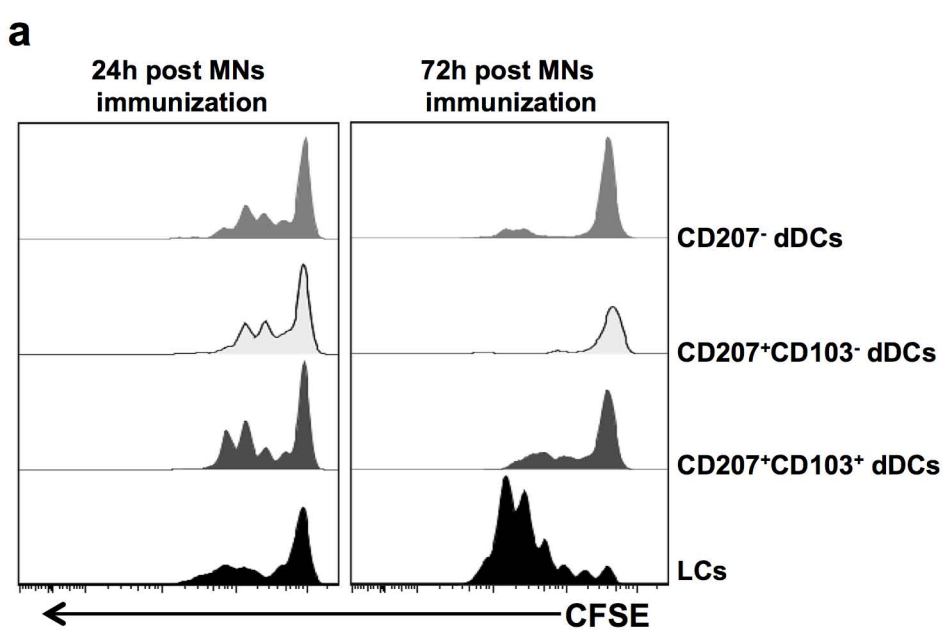
Figure 3: LCs promote Th1 and Th17 CD4⁺ T cell differentiation. DT-untreated or treated Lang^hDTR mice received *i.v.* 10^6 CD45.1 OT-II cells. Mice were immunized with b-NPs or OVA-NPs the following day and skin-draining LNs were harvested 7 days later. **a**) Percentages and total numbers of CD45.1⁺CD4⁺T cells recovered within each experimental group are shown. **c**) Total LN cells were re-stimulated with PMA-Ionomycin prior to intracellular staining. The expression of IFN-γ and IL-4 among CD4⁺CD45.1⁺ gated cells is shown. **c**) The same as in **b)**, but the expression of IL-17 and Foxp3 among different experimental groups is shown. **d**) Total numbers (mean ± SEM, n=6/group) of IL-4, IFN-γ, IL-17, IL-10 or Foxp3 expressing OT-II cells within each group.
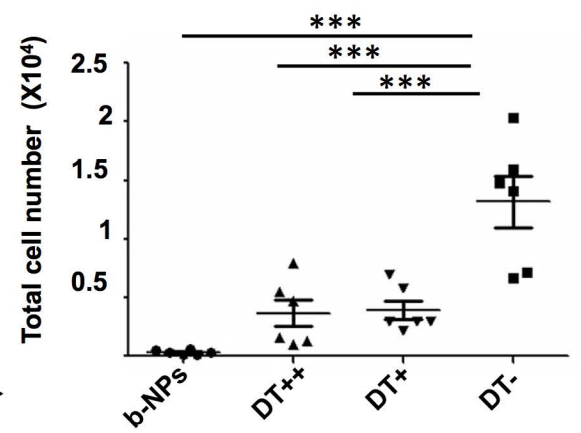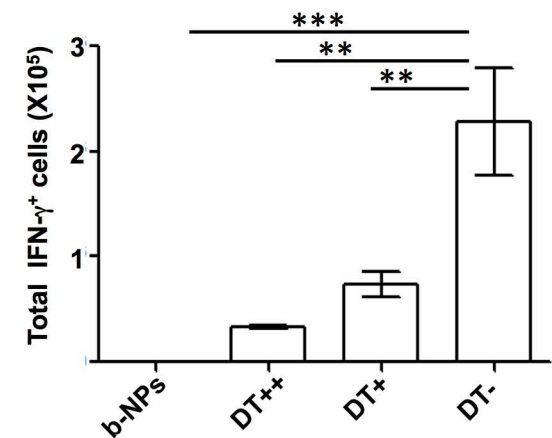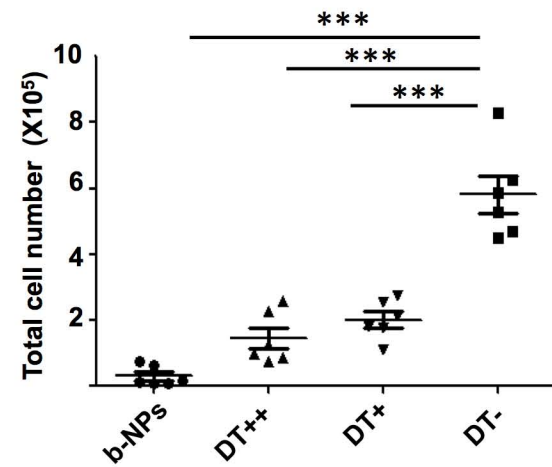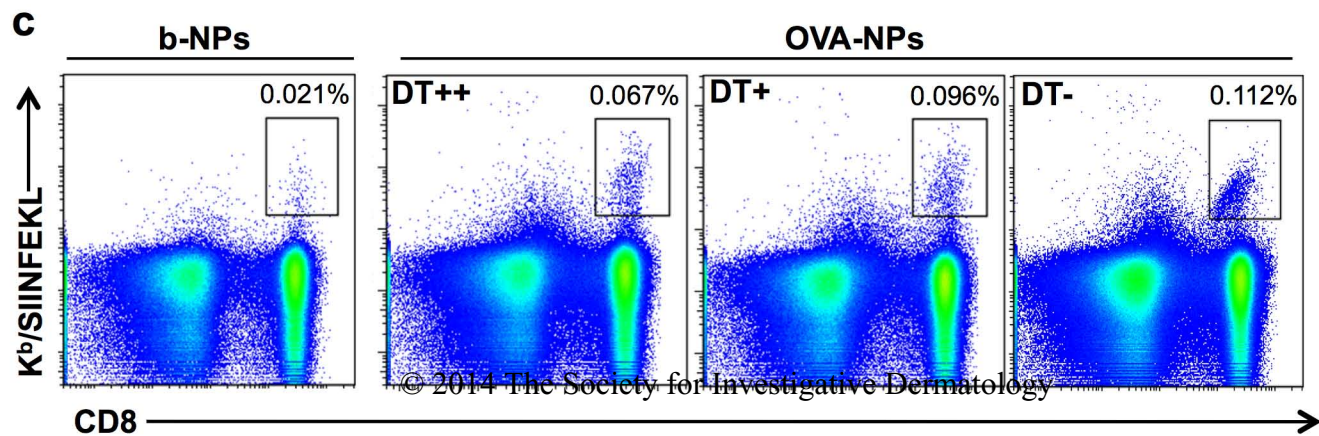
Figure 4: LCs are necessary for efficient anti-tumour responses. Lang^hDTR mice were DT-treated or untreated and immunized with b-NPs or OVA-NPs MNs. Three weeks later, mice were inoculated s.c. with B16.OVA melanoma cells. **a**) Tumour volume measurements (±SEM, n=9/group) over 18 days among experimental groups. **b**) As in **a**, but percentages of survival among different groups are shown. **c**) Percentages of OVA-specific, among tumour infiltrating CD8⁺ T cells, between experimental groups are shown. **d**) Lang^hDTR mice, DT-treated or untreated, were injected *s.c.* with 10^5 B16.OVA cells, and 4 and 9 days later, immunized with b-NPs or OVA-NPs. Tumour volumes (±SEM) among different treatment groups over 15 days post-inoculation are shown. **e**) As in **d**, but percentages of survival among treatment groups (n=9/group) are shown.

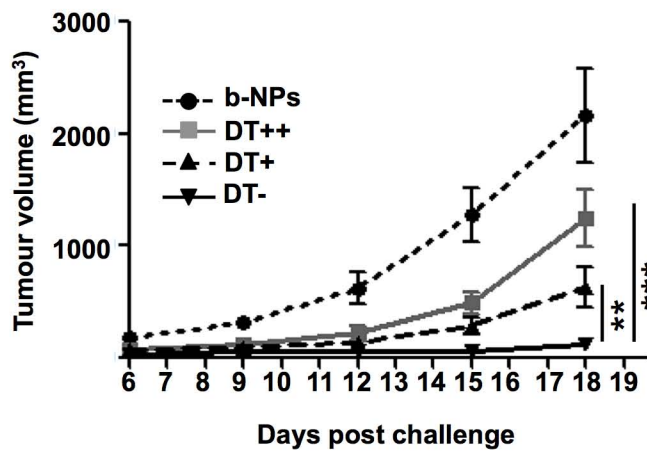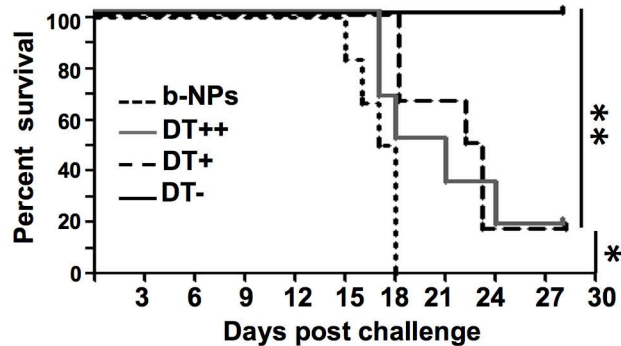**Figure 5: LCs are required for effective anti-viral immunity a**) Lang^hDTR mice, either DT-untreated or treated, were immunized with b-NPs or OVA-NPs MNs. Mice were challenged *i.n.* with SeV^OVATdT 3 weeks later. Survival among experimental

groups following SeV^{OVATdT} challenge (n=8-10/group) is shown. **b**) Representative dot-plots indicating percentages of SeV^{OVATdT} positive cells in total lung cell suspensions between groups 6 days post-infection. **c**) Bars indicating percentage of SeV^{OVATdT} positive cells in total lung cell suspensions between groups (n=10/group). **d**) Viral titres in lung homogenates between groups at 6 days post-infection. **e**) Percentages of OVA-specific CD8$^+$T cells infiltrating the lungs between immunization groups. **f**) IFN-γ and/or Granzyme B production following PMA/Ionomycin re-stimulation of OVA-specific CD8$^+$T cells infiltrating the lungs, as analysed 6 days post SeV^{OVATdT} challenge.

Figure 6: CD207$^+$CD103$^+$ dDCs preferentially cross-present soluble antigen delivered following microneedle immunization. Mice (n=20/group) were immunized through MNs with OVA-NPs or soluble OVA, and following 72h defined subsets of DCs from auricular LNs of both immunization groups were purified by FACS. 3-5x10^4 OVA-specific CD8$^+$ T cells were co-cultured in triplicates with 3-5x10^3 DCs of each subset for 60h. **a)** Representative histograms of CFSE dilutions of OT-I cell proliferation among both immunization groups are shown. **b)** Bars graphs representing the percentage of proliferating OT-I T cells. Data have been pooled from two separate experiments and are represented as mean ± SEM.

a

24h post MNs immunization | 72h post MNs immunization

CD207⁻ dDCs

CD207⁺CD103⁻ dDCs

CD207⁺CD103⁺ dDCs

LCs

CFSE

b

□ 24h post MNs immunization
■ 72h post MNs immunization

% of divided CD8⁺ T cells

*** / ** / *

CD207⁻ dDCs | CD207⁺CD103⁻ dDCs | CD207⁺CD103⁺ dDCs | LCs

c

24h post MNs immunization | 72h post MNs immunization

CD207⁻ dDCs

CD207⁺CD103⁻ dDCs

CD207⁺CD103⁺ dDCs

LCs

CFSE

d

□ 24h post MNs immunization
■ 72h post MNs immunization

% of divided CD4⁺ T cells

CD207⁻ dDCs | CD207⁺CD103⁻ dDCs | CD207⁺CD103⁺ dDCs | LCs

© 2014 The Society for Investigative Dermatology

© 2014 The Society for Investigative Dermatology

a

b-NPs | OVA-NPs

CD45.1 (y-axis), CD4 (x-axis)

b-NPs: 0.089%
DT++: 2.76%
DT+: 2.83%
DT-: 2.98%

b

Total cell number ($\times 10^5$)

b-NPs, DT++, DT+, DT-

* * ***

c

b-NPs | OVA-NPs

Isotype | b-NPs | DT++ | DT+ | DT-

IL-4 (y-axis), IFN-γ (x-axis)

Isotype: 0% / 0% / 99% / 0.3%
b-NPs: 0% / 0% / 98.7% / 1.3%
DT++: 1.66% / 0.1% / 92.7% / 5.5%
DT+: 0.34% / 0.02% / 92.2% / 7.4%
DT-: 0.2% / 0.07% / 81.2% / 18.5%

IL-17 (y-axis), Foxp3 (x-axis)

Isotype: 0.01% / 0.02% / 99.7% / 0.24%
b-NPs: 0.36% / 3.2% / 92.1% / 4.3%
DT++: 2.29% / 0.32% / 96.3% / 1.07%
DT+: 3.49% / 0.23% / 94.1% / 2.49%
DT-: 6.34% / 0.22% / 92.4% / 1.07%

© 2014 The Society for Investigative Dermatology

d

Total cell number ($\times 10^4$)

IL-4, Foxp3, IFNγ, IL-17

b-NPs, DT++, DT+, DT-

*** *** *** *** ** ***

a

b

c

b-NPs

OVA-NPs

DT++ 2.78%   DT+ 5.28%   DT- 14.2%

2.02%

K^b/SIINFEKL →

CD8 →

d

e

© 2014 The Society for Investigative Dermatology

a

Percent survival

- - - - b-NPs
———— DT++
- - - DT+
———— DT-

Days post challenge

b

b-NPs · OVA-NPs

SeV^OVA / TdT → / SSC →

b-NPs: 28.1%, DT++: 19.3%, DT+: 4.32%, DT-: 0.46%

c

% of infected cells

b-NPs, DT++, DT+, DT-

e

b-NPs · OVA-NPs

K^b/SIINFEKL → / CD8 →

8.58%, b-NPs: 8.58%, DT++: 14.2%, DT+: 19.5%, DT-: 28.3%

d

SeV^OVA / TdT titre log$_{10}$ ffu/ml

b-NPs, DT++, DT+, DT-

f

Isotype · b-NPs · OVA-NPs

IFNγ → / Granzyme B →

Isotype: 0.7%, 0%, 98%, 1.2%
b-NPs: 3.3%, 5.1%, 17%, 75%
DT++: 35%, 5.5%, 49%, 11%
DT+: 30%, 5.7%, 46%, 18%
DT-: 32%, 6.8%, 48%, 13%

© 2014 The Society for Investigative Dermatology

a

OVA-MNs   OVA-NPs MNs

CD207⁻DDCs

CD207⁺ CD103⁻DDCs

CD207⁺ CD103⁺ DDCs

LCs

CFSE

b

% of divided CD8⁺ T cells

- LCs
- CD207⁺CD103⁺ dDCs
- CD207⁺CD103⁻ dDCs
- CD207⁻ dDCs

OVA   OVA-NPs   OVA   OVA-NPs   OVA   OVA-NPs   OVA   OVA-NPs